

# INVESTIGATING THE ACOUSTIC PROPERTIES OF THE UNDERWATER IMPLOSIONS OF LIGHT GLOBES AND EVACUATED SPHERES

Alessandro Ghiotto<sup>1</sup>, Prof J.D. Penrose<sup>2</sup>

1. Nautronix, Ltd. 2. Centre for Marine Sciences and Technology, Curtin University

## Abstract

The dynamics of empty and gas filled cavities are reviewed from which estimations are made about source levels and spectra for cavities of particular size, depth and internal gas type and pressure. Household light globes and specially manufactured evacuated spheres were imploded at depths of 1m to 40 m and the pressure-time series and spectra of the implosions are presented.

The internal pressures of the unbroken vessels are estimated based on the bubble resonance frequency and implosion depth. Source levels and bubble resonance frequencies obtained from experimental results are compared with theoretical results derived from implosion depth and estimated initial internal gas pressure. The observed variability in source level, bubble resonance frequency and the presence of sub harmonics of the bubble resonance frequency are discussed.

## Introduction

Household light globes have been used with increasing popularity as an acoustic source. Unlike an airgun source, the initial gas pressure in the bubble is much lower than the ambient pressure and the bubble reaches equilibrium after a small number of oscillations. (The bubble pulse is less than 100 ms at 40 m.) The peak pressure developed is typically around 150 dB re 1  $\mu$ Pa for implosions at 40 m depth. Higher peak levels may be obtained by using vessels with a lower internal gas pressure. A low gas pressure also results in a short bubble pulse which is desirable for easier deconvolution of received signals and their associated multipaths, but shortening the pulse causes the energy to be distributed over a wider frequency band. Glass spheres with very low internal gas pressure were used as an alternative to light globes to investigate the effect of a lower internal gas pressure on radiated spectra and pulse duration.

## Bubble Dynamics

### The Rayleigh Collapse

Assuming sphericity at all times, the collapse of a vacuous cavity in an *incompressible fluid* was determined by Rayleigh (1917). The work done by the hydrostatic pressure in contracting the radius of an empty cavity from a maximum (starting) radius  $R_m$  to an instantaneous radius  $R$  is equivalent to the kinetic energy of the liquid. The kinetic energy of the liquid can be predicted by integrating the spherically symmetrical energy distribution over shells of liquid of thickness  $\Delta r$ , mass  $4\pi r^2 \rho \Delta r$ , and speed  $dr/dt$ . The work

done by the hydrostatic pressure  $p_0$  is  $(4/3)\pi p_0 (R_m^3 - R^3)$ . Maintaining that the fluid is incompressible, at any time  $\Delta t$ , liquid of mass  $4\pi r^2 \rho r \Delta t$  flows across the surface with radius  $r$ . Considering the flow at the cavity boundary,

$$\frac{\dot{r}}{\dot{R}} = \frac{R^2}{r^2} \quad (1)$$

The kinetic energy can now be evaluated as  $2\pi\rho\dot{R}^2 R^3$ .

The wall velocity,  $\dot{R}$  can be found to be:

$$\dot{R} = \pm \sqrt{\frac{2p_\infty}{3\rho} \left( \frac{R_m^3}{R^3} - 1 \right)} \quad (2)$$

The positive and negative roots correspond to the expanding and collapsing cavity respectively. Integrating the wall velocity with respect to time gives the collapse time.

$$t_{ray} = \int_{R_m}^0 \frac{1}{\dot{R}} dR \approx 0.915 \sqrt{\frac{\rho}{p_\infty}} \quad (3)$$

Withholding the assumption of an incompressible fluid, the derivation breaks down as  $dR/dt$  approaches the speed of sound in the liquid. This can be seen from equation (3), where as  $R$  becomes very small, the collapse speed becomes very large until finally when  $R=0$ , the result is undefined.

### Collapse of a Cavity Containing Gas

The gas inside a cavity will be compressed as the cavity collapses, thus retarding the collapse. The cavity will reach a minimum volume at some maximum gas pressure and then expand again until the gas pressure is well below the ambient liquid pressure and then collapse again, oscillating about some equilibrium

volume. Assuming no heat flow or dissipation, the gas pressure may be expressed as

$$p_g = p_{g,m} \left( \frac{R_m}{R} \right)^{3\gamma} \quad (4)$$

where  $\gamma$  is the ratio of specific heats of the gas in the cavity. The energy calculations now include the compression of the gas (which has pressure  $p_{g,m}$ ), represented by the last term in the conservation of energy equation (5). Assuming surface tension and vapour content is minimal and the external pressure  $p_0$  is constant, the energy equation for the bubble collapse is:

$$\frac{3\rho\dot{R}^2}{2} = p_0 \left[ \left( \frac{R_m}{R_{\min}} \right)^3 - 1 \right] - p_{g,m} \frac{1}{1-\gamma} \left[ \left( \frac{R_m}{R} \right)^3 - \left( \frac{R_m}{R} \right)^{3\gamma} \right] \quad (5)$$

The positions of maximum and minimum cavity radius are at  $R_m$  and at  $R_{\min}$ , at which time  $dr/dt = 0$ . At the minimum radius, equation 5 can be simplified to

$$p_{g,m} \left( \frac{R_m}{R} \right)^{3(\gamma-1)} = p_0(\gamma-1) \quad (6)$$

The minimum radius is then:

$$R_{\min} = \frac{R_m}{\left( \frac{p_0(\gamma-1)}{p_{g,m}} \right)^{\frac{1}{3(\gamma-1)}}} \quad (7)$$

### The Oscillating Bubble

Continuing with the assumption of a spherical bubble in an ideal fluid, a simple analogy can be made between the pulsating bubble and a bob of mass  $m$  attached to a spring. Using this analogy the stiffness, resonant frequency and the energy of the oscillator can be determined. The restoring force arises from the compressibility of the gas in the cavity and the inertia of the system is associated primarily with the moving liquid. The main flow of energy is between potential and kinetic energy, which is dependent on the acceleration of the bubble volume.

The bubble wall describes a motion  $R_\epsilon = -R_{\epsilon 0} e^{i\omega t}$  about a mean radius  $R_0$  and with resonance frequency  $\omega_0$  and displacement  $R_{\epsilon 0}$ . The kinetic energy of the liquid is then:

$$\phi_K = \frac{1}{2} \int_R^\infty (4\pi r^2 \rho dr) \dot{r}^2 \quad (8)$$

which may be expressed as  $\phi_K = 2\pi R^3 \rho \dot{R}^2$ .  $\phi_K$  is at a maximum at the equilibrium bubble radius  $R_{\epsilon 0}$ . At this position,  $dr/dt$  is also at a maximum, hence

$$|\dot{R}|^2 = (\omega_0 R_{\epsilon 0})^2 \quad (9)$$

$$\text{i.e. } \omega_0 = \frac{\dot{R}}{R_{\epsilon 0}} \quad (10)$$

Using the bubble energy equation (5) it can be shown that

$$\omega_0 = \frac{1}{R_0} \sqrt{\frac{3\gamma p_0}{\rho}} \quad \text{Minnaert (1933)} \quad (11)$$

This resonance frequency  $\omega_0$  requires that heat exchanges and surface tension effects are negligible. This has been shown to be an adequate approximation for bubbles as small as 1mm in diameter. (Leighton, 1997).

If the pulsating bubble is considered to behave as a harmonic oscillator, the 'spring stiffness' must be defined: Consider a bubble in a liquid of static pressure  $p_0$  which collapses from an equilibrium volume of  $V_0$  by  $\partial V$  to  $V$ , so the radius changes from  $R_0$  to  $R_0 - R_\epsilon$ . The gas pressure therefore increases from  $p_{i,e} = p_0 + 2\sigma/R_0$  by  $\partial p_i$  to  $p_i$ .

If  $p_i V^\kappa = \text{a constant}$  then

$$\Delta p_i = -\frac{\kappa}{V_0} p_{i,e} \Delta V \quad (12)$$

If  $R_\epsilon \ll R_0$  then  $\partial V = 4\pi R_0^2 R_\epsilon$

$$\text{and } \frac{\Delta V}{V_0} = -\frac{3R_\epsilon}{R_0} \quad (13)$$

The force necessary to change the bubble volume is due to the excess pressure acting over the surface area of the bubble. Using equations 12 and 13;

$$F_A = 4\pi R_0^2 \Delta p_i = -12\pi\kappa R_0 p_i R_\epsilon \quad (14)$$

The stiffness of the bubble can now be written as

$$k = 12\pi\kappa R_0 p_{i,e} \quad (15)$$

If the surface tension is omitted, then

$$k \approx \frac{3\kappa p_0}{R_0} \quad (16)$$

The inertia of the system is provided by the fluid mass flux in the vicinity of the pulsating cavity. This mass flux can be expressed as

$$\begin{aligned} Q &= \rho \frac{\partial Vol}{\partial t}(t) \\ &= \rho 4\pi R_0^2 \frac{\partial R}{\partial t} \end{aligned} \quad (17)$$

Hence the equivalent mass of the system is 3 times the mass of the water displaced by the bubble at equilibrium.

$$\text{i.e. } m_e = \rho 4\pi R_0^3 \quad (18)$$

### Damping

The formulas shown above describe a bubble which pulsates as a harmonic oscillator with no damping. The bubble is subject to damping, which is manifested in three ways:

- Energy radiated from the bubble in acoustic waves (radiation damping)
- Energy lost through thermal conduction between the gas and the surrounding liquid

- Work done against the viscous forces at the bubble wall (viscous damping)

The damping constant  $\delta$  is defined for damping at the resonance frequency as  $\delta = 1/Q$ , where  $Q$ , the Quality factor, is  $\omega_0 / (\frac{1}{2} \text{ power bandwidth})$ .

The decay of bubble oscillations due to the radiation of sound energy is independent of bubble size, unlike thermal and viscous damping which increase with decreasing bubble size. The loss factor due to radiation is equal to the radiation efficiency of the vibrating sphere.

$$\text{i.e. } b_{rad} = \frac{R_r}{\sqrt{R_r^2 + X_r^2}} = \frac{kR_0}{\sqrt{1 + (kR_0)^2}}$$

$$\text{where } k = \frac{2\pi}{\lambda}$$

$$\therefore kR_0 = \frac{\omega_0 R_0}{c} = \frac{R_0}{c} \frac{1}{R_0} \sqrt{\frac{3\gamma p_0}{\rho}} = \sqrt{\frac{3\gamma p_0}{\rho c^2}}$$

$$\text{If } kR_0^2 \ll 1$$

$$\text{then } \delta_{rad} = kR_0^2 = \sqrt{\frac{3\gamma p_0}{\rho c^2}} \quad (19)$$

As the bubble pulsates, more work is done by the liquid compressing the bubble than by the gas expanding the bubble. For energy to be conserved, energy must be released from the gas into the liquid upon expansion, and this is manifested in heat energy. This loss of heat energy to the liquid represents thermal damping. For an ideal gas where  $PV^\kappa = \text{constant}$  and  $TV^\kappa = \text{constant}$

$$d_{th} = \frac{3(\gamma - 1)}{R_0/l_D} \quad (20)$$

where  $l_D$  is the thermal boundary layer thickness and  $R_0/l_D \geq 5$

At the resonant frequency  $\omega_0$ ,

$$\frac{R_0}{l_D} = R_0 \sqrt{\frac{2\omega_0}{D_g}}$$

$$D_g = \frac{K_g}{\rho_1 C_p}$$

and  $K_g$  is the thermal conductivity of the gas,  $\rho_1 C_p$  is the specific heat capacity of the gas for a constant pressure.

The Navier-Stokes Equation for a fluid of constant viscosity is

$$\begin{aligned} \rho \frac{D\vec{v}}{Dt} &= \rho \left[ \frac{\partial \vec{v}}{\partial t} + (\vec{v} \cdot \nabla) \vec{v} \right] \\ &= \rho \Sigma \vec{F}_{ext} - \nabla p + \frac{\eta}{3} \nabla (\nabla \cdot \vec{v}) + \eta \nabla^2 \vec{v} \end{aligned} \quad (21)$$

If the fluid is incompressible then  $\vec{v} \cdot \nabla = 0$  and if the fluid is irrotational then  $\nabla^2 \vec{v} = 0$ , so equation (21) reduces to

$$\rho \frac{D\vec{v}}{Dt} = \rho \left[ \frac{\partial \vec{v}}{\partial t} + (\vec{v} \cdot \nabla) \vec{v} \right] = \rho \Sigma \vec{F}_{ext} - \nabla p \quad (22)$$

This suggests that there are no net viscous forces acting in an incompressible viscous liquid around the pulsating spherical bubble. Momentum transfer does occur through viscosity, but no *net* viscous force acts within the body of the liquid. Net viscous forces do occur at the bubble wall, where they result in an excess pressure. Volume elements at the bubble wall decrease in thickness and increase laterally as the bubble expands. In an incompressible fluid, these distortions must be the result of viscous stresses. As a result, there is an energy loss on compression. The viscous damping coefficient was derived by Devin (1959) as

$$\delta_{vis} = \frac{b_{vis}}{\omega_0 m_{rad}} = \frac{4\eta}{R_0^2 \rho \omega_0} \quad (23)$$

$$\text{where } b_{vis} = \frac{\eta}{\pi R_0^3}$$

#### Total Damping Constant

The damping contributions due to radiation, heat and viscous losses are additive. The total damping constant at resonance is therefore:

$$\delta_{tot} = \frac{R_0 \omega_0}{c} + \frac{3(\gamma - 1)}{R_0 \sqrt{\frac{2\omega_0 (\rho_1 C_p)}{K_g}}} + \frac{4\eta}{R_0^2 \rho \omega_0} \quad (24)$$

#### Pressure Radiated by a Spherical Pulsating Bubble

Firstly, consider the pressure radiated by a cavity with a non-varying internal pressure, so that the radiated acoustic pressure is governed by the interface movement only. The motion of the cavity wall may be described by

$$\begin{aligned} R &= R_0 - R_\epsilon e^{i\omega t} \\ \dot{R} &= -i\omega R_\epsilon e^{i\omega t} = U_0 e^{i\omega t} \\ \ddot{R} &= i\omega U_0 e^{i\omega t} \end{aligned} \quad (25)$$

where the frequency of oscillation is  $\omega$  and the amplitude is  $U_0$ .

The pressure at the bubble wall varies with time as

$$P(r, t) = \rho_0 c U_0 e^{-\beta(t-r/c)} \frac{R_0}{r} \cos(\chi_0) e^{i(\omega t - k(r-R_0) + \chi_0)} \quad (26)$$

where  $\beta$  relates to the damping constant, such that

$$\beta = \frac{\delta_{tot}}{2m}$$

and  $\chi_0$  relates to the phase of the pressure wave, such that

$$\cos \chi_0 = \frac{kR_0}{\sqrt{1 + (kR_0)^2}}$$

#### Considering Bubble Acceleration

Rearranging equation (5)

$$\dot{R}^2 = \frac{2p_0}{3\rho} \left[ \left( \frac{R_m}{R} \right)^3 - 1 \right] - p_{g,m} \frac{1}{1-\gamma} \left[ \left( \frac{R_m}{R} \right)^3 - \left( \frac{R_m}{R} \right)^{3\gamma} \right] \quad (27)$$

hence the acceleration during bubble compression

$$\ddot{R} = \frac{p_\infty R_m^3}{\rho} \left\{ \frac{p_{g,m}}{p_\infty} \frac{1}{(1-\gamma)} \left[ R^{-4} - \gamma R_m^{3(\gamma-1)} R^{-(3\gamma+1)} \right] \right\} \quad (28)$$

Substituting equation (5) into equation (25) yields

$$\ddot{R} = \frac{p_\infty}{R\rho} \left[ \frac{p_{g,m}}{p_\infty} \left( \frac{R}{R_m} \right)^{-3\gamma} - 1 - \frac{3\rho}{2p_\infty} \dot{R}^2 \right] \quad (29)$$

During expansion,  $R_m$  is the minimum radius, and  $p_{g,m}$  becomes  $p_{g,max}$ .

Vokurka (1985) relates equation (25) to the equilibrium radius:

$$\ddot{R} = \frac{p_\infty}{R\rho} \left[ \left( \frac{R}{R_0} \right)^{-3\gamma} - 1 - \frac{3\rho}{2p_\infty} \dot{R}^2 \right] \quad (30)$$

with initial conditions for  $R(t)$  being  $R(0) = R_{max}$  and  $\dot{R}(0) = 0$ .

Vokurka (1985) showed that the pressure in the liquid at the bubble wall, when observed in the far field, is

$$p_{bl}(t) = p(t) - p_\infty \approx \rho \frac{R}{r} (\ddot{R}R + 2\dot{R}^2) \quad (31)$$

## Experiment

Two experiments were conducted: one in the sheltered waters of Jerviose Bay, W.A in a water depth of 10m and another just west of Rottnest Island, WA, near the 100m contour. The light globes and glass spheres were imploded using the device shown in figure 1 which is similar in design to that described by Heard *et al*, (1997) and by Chapman *et al* (1977).

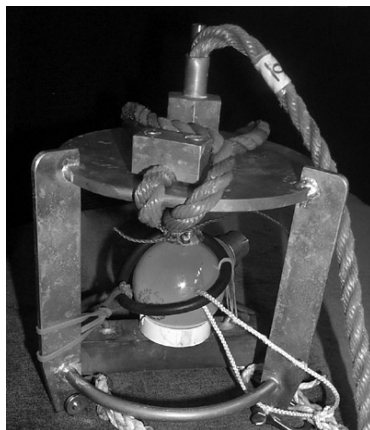


Figure 1 - Imploder device used to break light globes and evacuated spheres

## Data Acquisition

For both trials, the receiver used was a Brüel & Kjaer 8100 Hydrophone, with a sensitivity of  $-206$  dB. The signal was recorded on a Sony portable DAT recorder at 22050 Hz. The analog signal from the DAT was resampled at 22050 Hz using a PC soundcard. Levels were calibrated using a white noise source at 96.2 dB re  $1 \mu\text{Pa}$ . Maximum pressure levels were retrieved before any filtering was done. Signals were then Butterworth high pass filtered at 15 Hz to eliminate surge noise and other unwanted low frequency components. The power spectrum densities were then calculated using 14 bit FFT's, using a boxcar window of the same width, overlapped by half the window width. The spectra were then normalised to energy spectrum densities, referenced to  $1 \mu\text{Pa}^2/\text{Hz}^2$ . These curves were smoothed with a 5 point running average filter as the output was still very spiky. The resonant frequency was then located.

## Results

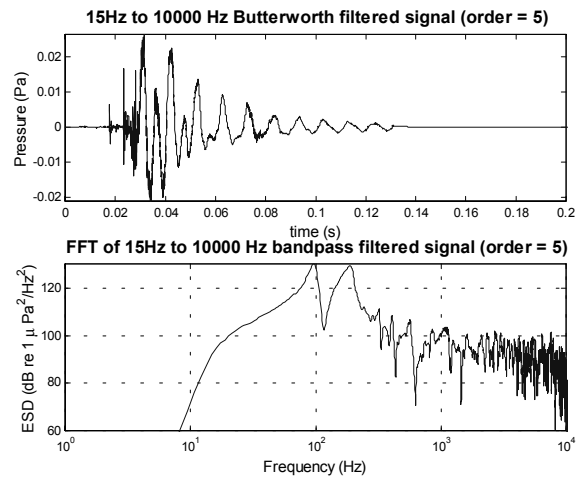


Figure 2 – Light globe at 5m depth

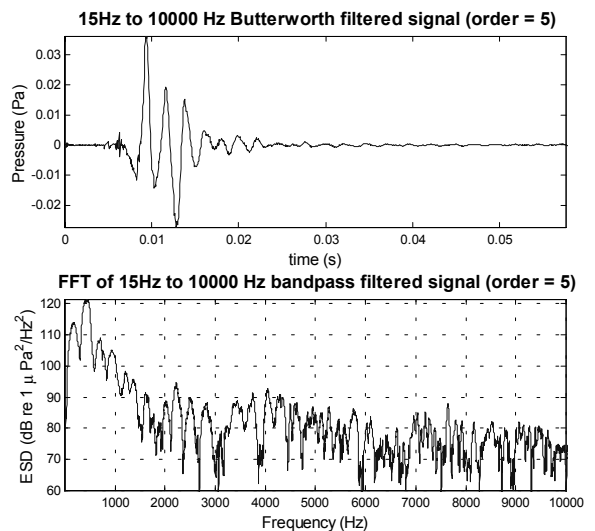


Figure 3 - Light globe at 40m depth

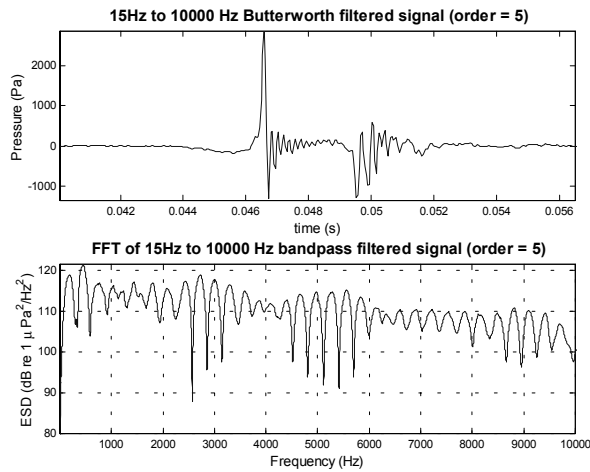


Figure 4 - Evacuated Sphere at 40m depth

If the resonant frequency is determined using Minnaert's (1933) equation, it is dependent on the equilibrium radius of the cavity, which may be found if the initial internal pressure of the cavity is known. For the theoretical resonant frequencies shown in Figure 5, an average of  $p_i$  the internal pressures for the light globes (except those greater than 1 atm) was used. This average was 55% of atmospheric pressure. Calculated resonant frequencies fall close to the measured values, indicating that the adiabatic assumption needed to determine  $p_i$  is adequate for gas filled cavities in seawater.

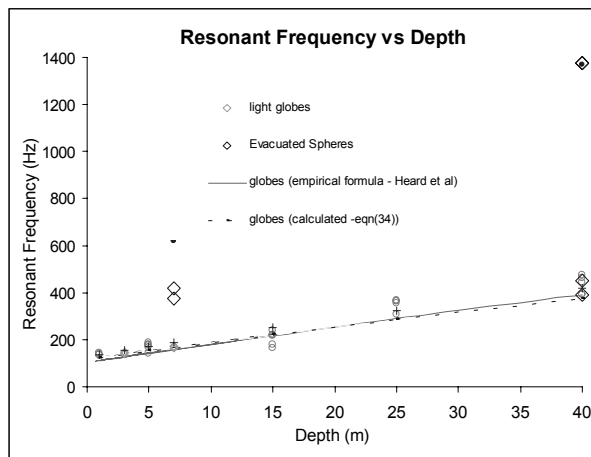


Figure 5 - Primary resonance of bubble oscillations as a function of depth.

This relationship can be found by applying the gas law  $p_i V_i^\gamma = p_0 V_0^\gamma$  to find  $R_0$  as a function of  $p_0$  and  $p_i$  and substituting into Minnaert's resonance equation.

$$i.e. \omega_0 = \frac{1}{p_i^{3\gamma} R_i} \sqrt{\frac{3\gamma p_0}{\rho}} \quad (32)$$

The value used for  $\gamma$  which gave resonant frequencies closest to those which were measured experimentally was  $\gamma = 1.40$ . This ratio of specific heats applies to diatomic gasses. If  $p_i$ ,  $R_i$  and  $\gamma$  remain constant for all  $d$ , then  $f_0$  is dependent on  $p_0$  only. Hence:

$$\begin{aligned} \therefore f_0 &\propto p_0^{\frac{1}{3\gamma}} p_0^{\frac{1}{2}} \\ i.e. f_0 &\propto p_0^{\frac{2+3\gamma}{6\gamma}} \\ i.e. f_0 &= k \left( \frac{d}{10} + 1 \right)^{\frac{3.1}{4.2}} \end{aligned} \quad (33)$$

where  $d$  is the depth in meters. The value for  $k$  can then be determined from the measured data as

$$\log(k) = \log(f_0) - \frac{3.1}{4.2} \log(p_0)$$

Using an average value for  $k$ , the resonant frequency was found to have depth dependence:

$$f_0 = 114 \left( \frac{d}{10} + 1 \right)^{\frac{3.1}{4.2}} \quad (\text{Hz}) \quad (34)$$

This relationship is shown as a dashed curve in Figure 5. The measured resonant frequencies were consistent with Heard *et al's* (1997) empirical formula for the resonant frequency of light globe implosions at a given depth:

$$f_0 \propto g(d+10)^{\frac{5}{6}} \quad (\text{Hz}) \quad (35)$$

Using  $g = 9.8 \text{ m/s}^2$  and  $d$  in meters, the constant of proportionality used in equation (32) was 2.5.

$$i.e. f_0 = 2.5 g(d+10)^{\frac{5}{6}} \quad (\text{Hz}) \quad (36)$$

This relationship is shown as a solid curve in Figure 5.

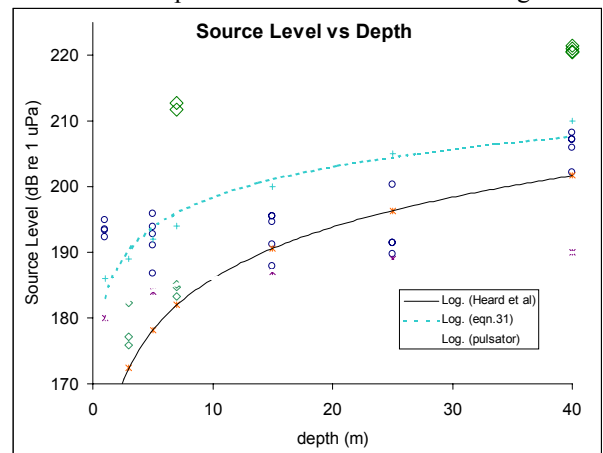


Figure 6 – Source Level vs. Depth

The equation used to calculate the peak pressures of the globes (equation (26)) is that of a rigid pulsator and

does not account for the changing pressure within the bubble. Predicted source levels using equation (26), illustrated by the hashed curve in figure 6, are within the lower limit of experimental values for light globes at depths no greater than 25m.

$$i.e. SL_{pulsator} = 180 + 5.25 \log(d) \text{ dB re } 1 \mu\text{Pa @ } 1\text{m}$$

The source levels derived from the measured peak pressures received due to light globe implosions varied by up to 10 dB at each depth, whereas the evacuated sphere levels varied by only 1 dB at 7m and at 40m. Predicted source levels for the evacuated spheres are 14 dB lower than measured levels at 7m and 20 dB below the measured levels at 40m. If internal pressure changes are taken into account and equation (31) is used to predict received levels, as illustrated by the dashed curve in figure 6 the predicted curve is much steeper than that which is indicated by Heard, *et al* (1997) or by the measured values. Using this model, the source level varies with depth as

$$SL_a = 183 + 15 \log(d) \text{ dB re } 1 \mu\text{Pa @ } 1\text{m}$$

Predicted evacuated sphere source levels, using this method, were overestimated by ~ 40 dB at 7m and at 40m.

### Predicting Bubble Motion

The source levels predicted by equation (31) are generally an overestimation of the measured levels, however an indication of the bubble radius as a function of time can be attained using equations (21), (25), (27), (29) and (30) from which the pressure equation is derived. Equations (25) describe the bubble's oscillation as simple harmonic. The damping factor of equation (24) is included in equation (26).

Bubble oscillations are not simple harmonic and bubble wall dynamics give rise to an asymmetry in the positive and negative pressure phases. This asymmetry, which is described by Rayleigh's equation for bubble oscillations, may be understood by applying energy conservation constraints to the system. Equation (5) describes this and the equation for the squared velocity of the bubble wall and equation (28) is a rearrangement of the energy conservation equation (5). Two models were used to simulate the implosions, one of which incorporated the adiabatic change in pressure within the bubble, and one which treated the bubble as a rigid pulsator. Peak pressure levels calculated using the rigid pulsator model were generally lower than the measured levels and those calculated using the more sophisticated model were *much* higher than measured levels.

The spectra shown in figures 2, 3 and 4 show an interesting harmonic structure, particularly in the case of the evacuated spheres. Part of this structure is likely

to be present at the source and due to harmonics of the bubble volume. Minnaert's (1933) resonance frequency is proportional to the equilibrium bubble radius and describes the principal resonance of a bubble of that size. It is unlikely that the bubble will collapse uniformly and remain always spherical. More probably, a cavity starting with a radius of 3 to 4 cm will collapse with multiple spherical harmonics (Leighton, 1997), as the surface tension effects (which act to retain sphericity) are not sufficient to dominate over external forces at these scale lengths. Each of these harmonics can be treated as a small bubble, with a resonant frequency and amplitude related to the order of the harmonic. Part of the harmonic structure is also due to interference from surface reflections of the signal, which arrive at the receiver out of phase with the direct signal.

For example, consider a source depth of 40m and a receiver depth of 3m, separated by a horizontal distance of 10m, as was the case for the evacuated spheres. The direct signal path has a length of 37.9m and the signal path which involves one surface reflection has a length of 43.8m. This difference means that signals with  $\lambda = n(43.8-37.9) = 4.9n$  will be attenuated due to destructive interference. This wavelength corresponds to multiples of 311 Hz at the measured sound speed of 1525 m/s. Figures 4 shows nulls occurring at multiples of 316 Hz, but other evacuated sphere spectra showed nulls occurring as low as 250 Hz. This variation may be attributed to the variation in receiver depth (and less significantly, source depth), induced by platform movement.

### Experimental Uncertainties

The environment at Jervoise Bay was very quiet in comparison to the open water off Rottneest Island where the second trial was undertaken. A great deal of low frequency noise appeared on the original signals from the second trial, which was filtered out. During this trial, the hydrophone was hung off the side of the boat and as the boat rolled and pitched, the hydrophone depth would vary, introducing flow noise and depth uncertainty. The receiver depth uncertainty was determined to be no greater than  $\pm 0.65\text{m}$ . A sea anchor was used to minimise drift. This contributed to flow noise as the drift rate was less than the current speed. The boat's hull is fiberglass, and the hydrophone cable was coupled directly to it. As waves interacted with the hull, noise was transmitted to the hydrophone via two channels: Transmission from the hull to the cable, and reflection from the hull to the hydrophone, only 3m away. Other noise sources which may have contributed were:

traffic: 1 large ship was observed to pass within approximately 2km of the experiment site

Biological noise – Snapping shrimp produce very loud impulsive clicks which may result in spikes in the observed signals. (A typical shrimp snap of 160 dB re 1  $\mu$ Pa @ 1m at 100m depth would result in a received level of approximately 120 dB re 1  $\mu$ Pa @ 1m.

These uncertainties in background noise levels can be minimised by measuring the average noise level over a period, calculating the spectrum density, and removing the components which are likely to interfere with results.

As seen in figure 1, the device used to implode the globes and spheres has a brass plate above the mount point for the globe. If the receiver is above the imploder and the depression angle is large then there will probably be significant reflection of the signal. This was the case for implosions off Rottneest Island at depths of 25m and 40m, and at Jervoise Bay for implosions at depths of 7m. The extent to which this reflection has altered the source from the assumed monopole has not been investigated. One solution is to remove the brass plate from the imploder and replace it with a structure similar to that on which the globe is mounted.

There was also a large uncertainty in the depth of the water column for those globes imploded at 1m, 5m, 15m and 25m during the second trial. Several light globes were imploded at 1m depth as depth sounders throughout the experiment, as the boat drifted. These implosions had insufficient energy for a bottom-reflected signal to be detected, but the implosions at 40m depth were sufficiently energetic. Distances calculated from the time delay between the direct signal and the first bottom reflection of the globes at 40m indicated depths of around 110m. i.e. Time difference between direct path and first bottom reflection of last light globe implosion at 40m (B.5.5) = 0.09s. The direct path length is approximately 38m, which at  $c = 1525$  m/s, equates to 0.025 s. This makes a total travel time of 0.115 s for the reflected path. This time is equivalent to 178m. Add 43m for the receiver depth and source depth and the result is twice the water depth, plus a small amount due to the source – receiver separation. These depths were also referenced from local charts using GPS measurements.

The internal pressures of the light globes, calculated from using Minnaert's resonance equation and ideal gas laws, was seen to vary from ~0.3 atm to ~0.9atm. The (expired) globes imploded at Jervoise Bay had internal pressures of around 0.75 atm, whereas those which were imploded off Rottneest, which were new, varied widely in predicted internal pressure. The measured resonant frequency for globes imploded off Rottneest Island was also quite variable at any given depth, and this variation gave rise to the variation in the predicted internal globe pressures. It is feasible that internal gas pressure of light globes may vary, as the

purpose of the gas is only to prevent the filament from being oxidised. An averaged internal pressure of 0.55 atm was used to model the depth dependence of source level and resonant frequency.

The spectra of globes imploded at 1m depth 1 globe which was imploded at 5m depth off Rottneest Island exhibited 2 strong peaks. The second of these was treated as the resonant frequency as it was consistent with predicted results. The first peak is possibly a subharmonic emission, which is possibly due to a prolonged expansion phase and a delayed collapse phase (Akulichev, 1967).

Other theories for subharmonics are described by Faraday (1831), Rayleigh (1883), Neppiras (1969), and others who describe surface waves which propagate at half the exciting frequency (due to the bubble oscillations).

Large bubble theory is summarised by Eller and Flynn (1969) wherein a threshold pressure exists for bubbles which may produce subharmonics at half the natural resonance

i.e.

$$P_{A2} = \frac{6p_0\Delta_{\log}}{\pi}$$

where  $\Delta_{\log}$  is the logarithmic decrement representing the damping of the oscillations.

Figure 2 shows a signal where it appears the bubble begins to collapse but then expands again before the collapse phase is completed. The process is repeated at least 4 times. This behaviour may be present at the source, in which case Akulichev's theory fits, or it may be due to surface reflections canceling out part of the signal at the correct phase. The difference in range between the direct path and the surface reflected path is 3.66m, which equates to 0.0024 s. The time difference between the observed double peaks occurs at intervals of ~ 0.025 s, ruling out surface reflections as the cause for this effect. The logarithmic decrement for this example is ~ 0.23, which corresponds to  $P_{A2} = 63845$  Pa, given that the implosion occurred at 5m depth. The recorded peak pressure was -358 Pa, at a range of approximately 8.5m. Accounting for attenuation due to spherical spreading, the source level was approximately 3160 Pa, well below Eller and Flynn's subharmonic threshold.

## Conclusions

The resonant frequency of light globe implosions was found to be in good agreement with Heard *et al* (1997)'s empirical equation, and fit well to theoretical models which employed Minnaert's resonance equation and assumed that the pulsation of the cavity volume was adiabatic.

Peak pressure levels varied by up to 9 dB over the sample tested and in order to find an empirical equation for the source level vs depth relationship samples are required over a greater range of depths. Heard *et al* (1997)'s empirical equation fit the data adequately well, although the data was spread sufficiently such that a linear fit would also have appeared to be good. A rigid pulsator model underestimated pressure levels as depth increased, where bubble wall acceleration is expected to be higher, and a model which incorporated bubble wall acceleration overestimated pressure levels.

Evacuated spheres were very consistent in peak pressure output at both depths at which they were tested and a pressure/depth relationship could be established given further tests at a range of depths.

Subharmonics were observed for implosion depths of 5m and Akulichev's (1967) large bubble theory may account for this.

## References

Akulichev, V.A., "The structure of solutions of equations describing pulsations of cavitation bubbles", *Akusticheskii J.* (Russian), 1967; 13: 533-537

Chapman, N.R., Jaschke, L, McDonald, M.A, Schmidt, H, Johnson, M, "Mitled field geoacoustic tomography experiments using light bulb sound sources in the Haro Strait Sea trial", *Oceans 1997 MTS/IEEE Conference Proceedings*, Vol. 2, Pt. 2

Devin, C.Jr, "Survey of thermal, radiation, and viscous damping of pulsating air bubbles in water", *JASA* 1959; 31:1654

Eller, A.I. & Flynn, H.G., "Generation of subharmonics of order one half by bubbles in a sound field", *JASA*, 1969; 46: 722-727

Faraday, M., "On the forms and states assumed by fluids in contact with vibrating elastic surfaces", *Phil Trans Roy Soc.*, 1831; 121: 319-340

Heard, G.J, McDonald, M, Chapman, N.R, Jaschke, L, "Underwater light bulb implosions: A useful acoustic source", *Oceans 1997 MTS/IEEE Conference Proceedings*, Vol. 2, Pt. 2

Leighton, T.,G., "The Acoustic Bubble", Academic Press, 1997, USA.

Minnaert, M., "On musical air bubbles and sounds of running water", *Phil Mag* 1933; 16: 235:248

Neppiras, E.A., "Subharmonic and other low frequency emission from bubbles in sound-irradiated liquids", *JASA*, 1969; 46: 587-601

Neppiras, E.A., "Subharmonic and other low frequency emission from sound-irradiated liquids", *J Sound Vib*, 1969; 10: 176

Rayleigh Lord, "On the pressure developed in a liquid during the collapse of a spherical cavity", *Phil Mag* 1917; 34: 94-98

Rayleigh Lord, "On the crispations of fluid resting upon a vibrating support", *Phil Mag Ser 5*, 1883; 16:50-58

Vokurka, K., "On Rayleigh's model of a freely oscillating bubble. I. Basic Relations", *Czech J Phys* 1985; B35: 28-40